

## Optical design of the general-purpose Spanish X-ray beamline for absorption and diffraction

G. R. Castro

European Synchrotron Radiation Facility, Avenue des Martyrs, BP 220, F 38043 Grenoble CEDEX, France, and Comisión Interministerial de Ciencia y Tecnología, Rosario Pino 14–16, 6a plta, E-28020 Madrid, Spain.  
E-mail: castro@esrf.fr

(Received 4 August 1997; accepted 2 December 1997)

This paper describes the optical design of the general-purpose Spanish beamline for absorption and diffraction (SpLine), which will be installed on a bending-magnet port of the ESRF. This beamline is planned to cover the needs of the Spanish synchrotron radiation community with broad scientific fields of interest, covering physics, chemistry, materials science and biology. By using the advantages of a wide front end (9 mrad), the Spanish beamline will be split into two branches. Both branches will be equipped with focusing optics and experimental stations. Thus, each branch can be operated simultaneously and independently from each other. One branch (*A*) will have two experimental stations, one for high-resolution powder diffraction (HRPD) and the other for X-ray absorption spectroscopy (XAS) and X-ray standing waves (XSW). The other branch (*B*) will have facilities for macromolecular crystallography and for single-crystal diffraction analysis, including that of surfaces and interfaces, as well as an X-ray diffraction/scattering camera for non-crystalline specimens.

**Keywords:** X-ray optics; multipurpose beamlines; beamline design.

### 1. Introduction

The main goal of the Spanish CRG X-ray beamline is to satisfy the needs of the Spanish scientific community with a broad range of interests across very different research areas. The beamline will be sited on the dipole BM25. A 9 mrad wide front-end centred at  $-7$  mrad will be used. The beamline will be split into two branches. Both branches will be fully equipped with focusing

optics and experimental stations. This design will permit measurements on either branch to proceed independently. Each branch will have two experimental stations with similar technical operations. One branch will be allocated on the soft edge (*A*) and the other on the hard edge (*B*) of the corresponding bending magnet. Branch *A* will be allocated the following facilities: high-resolution powder diffraction (HRPD) including anomalous dispersion; X-ray absorption spectroscopy (XAS) and X-ray standing waves (XSW). Branch *B* will be used for: macromolecular crystallography including multiple anomalous dispersion (MAD); single-crystal diffraction and diffraction from interfaces; X-ray diffraction/scattering camera for non-crystalline specimens.

### 2. Beamline

The planned beamline will be installed at a bending-magnet port, where the (lateral) dimension of the beam spot at the distance where the optical components should be located is around 5 cm. The planned beamline, as a multidisciplinary and multipurpose one, will be split into two branches and therefore for each branch corresponding optical elements will be constrained by the space availability and source characteristics (Hazemann *et al.*, 1995; Pascarelli *et al.*, 1996; Kirsch *et al.*, 1991). The beamline optics have been designed to fit the users requirements and preserve the exceptional characteristics of the source. A general layout of the planned beamline is shown in Fig. 1.

#### 2.1. Source characteristics

The beam will be split into two branches, considering the variation of the critical energy (magnetic field) across a horizontal fan of the bending magnet and maximizing the separation between them. Fig. 2 shows the angular profile of the critical energy over the total angular acceptance on the beamline front end. Two different plateaus can be distinguished, each with approximately 4 mrad horizontal opening angle. It has been decided to split the beam into two fans of 2 mrad each, with the central 5 mrad blocked. The hatched zones in Fig. 2 correspond to the two regions selected for the beamlines. Branch *A* with a critical energy of 9.6 keV is centred on  $-3.5$  mrad and branch *B* with a critical energy of 20.6 keV is centred on  $-10.5$  mrad. Therefore, the corresponding angular apertures are  $[-2.5 -4.5]$  mrad and  $[-9.5 -11.5]$  mrad, respectively.

#### 2.2. Optics

The optical paths in both branches are shown in Figs. 3(a) and 3(b). Owing to the multipurpose and interdisciplinary char-

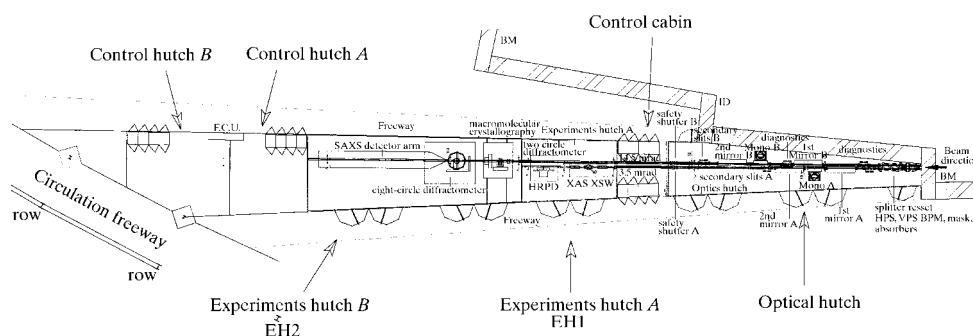


Figure 1  
General beamline layout.

**Table 1**  
Characteristic parameters of the optical design of branch A.

Optical elements	First mirror Two strips Rh and Pt coated	Monochromator Pseudo channel-cut type Si(111) or Si(311)	Second mirror Two strips Rh and Pt coated
Distance from source	~27.0 m	~28.5 m	~30.0 m
Focusing type	Vertical collimation	Dynamical sagittal focusing	Vertical focusing
Horizontal acceptance	2 mrad		
Spectral range	4–35 keV		
Energy resolution ( $\Delta E/E$ )	$1.5 \times 10^{-4}$ – $4.0 \times 10^{-5}$		
Flux at sample (beam current 0.1 A)	$\sim 10^{12}$ photons $s^{-1}$		
Nominal beam size at	40 m ( $A_1$ )	45 m ( $A_2$ )	
Vertical phase space	224 $\mu\text{rad} \times 0.09$ mm	154 $\mu\text{rad} \times 0.09$ mm	
Real space ( $H \times V$ )	0.07 $\times$ 0.09 mm	20.14 $\times$ 0.08 mm	
Vertical magnification ( $m_V$ )	0.40	0.58	
Horizontal magnification ( $m_H$ )	0.37	0.56	

acteristic of the planned beamline, the chosen optics should be as flexible as possible and should accept a 2 mrad horizontal aperture and produce a small focal spot at different sample positions. The optics for each branch consist of two mirrors and a fixed-exit double-crystal monochromator (DCM). The beam can be focused to different sample positions away from the source by a vertically focusing mirror (second mirror) having a variable bending radius. The horizontal focusing will be achieved by the second monochromator crystal through a sagittal cylindrical bending (Heald, 1984; Pascarelli *et al.*, 1996). All optical components of the beamline will be operated under vacuum. A fixed Be (500  $\mu\text{m}$ ) window at the front end will be used to separate the beamline and the electron ring as a preventative measure. In order to reduce the influence in the region of low energy (increasing the real cut-off energy), vacuum gate valves with a beryllium disc will be used to separate the different components. In some special cases, if necessary and if the vacuum conditions are good, the Be windows can be opened for maximum flux. For example, at 4 keV operation, it is very important to minimize the thickness of Be between the source and the sample. At this energy, a Be foil of 1500  $\mu\text{m}$  reduces the transmission by a factor of ten. Tables 1 and 2 list the most relevant parameters of the chosen optical design.

In the case of branch A, the first mirror will be located at ~27 m from the source. This mirror (collimating mirror) will have two functions, primarily to suppress the higher-order harmonics of the energy selected while totally reflecting the useful energy and to reduce heating of the subsequent optical element and, secondly, to collimate the vertical divergence of the beam in order to optimize its energy resolution, which would be determined only by the Darwin width of the first crystal of the monochromator. This mirror with a constant curvature radius  $R_V = 21.6$  km will be coated with Rh and Pt (two strips). The angle of incidence will be set at 2.5 mrad, which corresponds to a cut-off energy of 26.8 keV for the Rh coating and 33.7 keV for Pt. The spectral energy range will be 4–35.0 keV. Owing to the high power loads of the ESRF beams (~150 W), cooling of the mirror is mandatory.

The monochromator chosen for both branches is of the pseudo channel-cut type (fixed exit) with two fixed Si(111) crystals moved together by a simple goniometer circle in the  $(-n, +n)$  configuration. Changing both crystals on the monochromator according to resolution requirements [e.g. Si(311)] is also possible. The first monochromator crystal should be water cooled while the second will be kept at room temperature. The second

crystal will be equipped with a piezoelectric driver that will allow its Bragg angle (pitch adjustment) to change very slightly to reduce the harmonic content of the beam, if necessary, and to keep the transmission of the monochromator constant during long time intervals. Also, a bender will curve sagittally this crystal in order to dynamically focus the beam at the different sample positions (Heald, 1984; Pascarelli *et al.*, 1996). The monochromator will be located at distances of around 28.5 and 32.0 m from the source for branch A and branch B, respectively. For a sample-to-monochromator distance of 40 to 50 m, the cylinder curvature radius ( $R_S$ ) will be varied between 0.9 and 22 m, depending of the photon energy setting (Bragg angle). The position and dimension of the focused beam will be kept constant during an ~1 keV energy scan, standard in an EXAFS measurement. The technical requirements of the monochromator of branch B are relatively simple compared to those of branch A since the measurements will be performed at a constant energy. Therefore, dynamical focusing will *not* be necessary. Energy scans around an absorption edge with moderate stability will only be necessary in the case of anomalous scattering. The Si(111) Darwin width meets the bandwidth necessities for resonant anomalous-scattering measurements. In the case of branch A, the optical system moves the focused X-ray beam downwards; in branch B, the beam is moved upwards. This enables space to be gained at the sample position in the experimental hutch A.

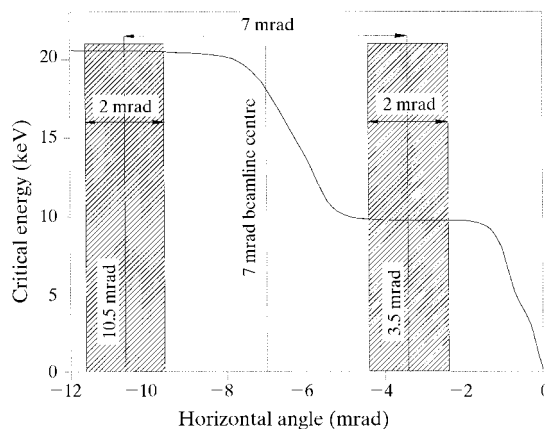


**Figure 2**  
Angular profile of the critical energy on the wide front end

**Table 2**  
Characteristic parameters of the optical design of branch *B*.

Optical elements	First mirror Two strips Rh and Pt coated	Monochromator Pseudo channel-cut type Si(111)	Second mirror Two strips Rh and Pt coated
Distance from source	29.0 m	32.0 m	33.5 m
Focusing type	Flat	Sagittally focusing	Vertically focusing
Horizontal acceptance		2 mrad	
Spectral range		6–35 keV	
Energy resolution ( $\Delta E/E$ )		$4 \times 10^{-4}$ at 1 Å	
Flux at sample (beam current 0.1 A)		$10^{12}$ photons $s^{-1}$	
Nominal beam size at	48 m ( $B_1$ )	50.5 m ( $B_2$ )	57 m ( $B_3$ )
Vertical phase space	167 $\mu\text{rad} \times 0.09$ mm	143 $\mu\text{rad} \times 0.10$ mm	103 $\mu\text{rad} \times 0.12$ mm
Real space ( $H \times V$ )	0.10 $\times 0.09$ mm	0.09 $\times 0.10$ mm	0.13 $\times 0.12$ mm
Vertical magnification ( $m_V$ )	0.43	0.52	0.70
Horizontal magnification ( $m_H$ )	0.50	0.58	0.78

The second cylindrical bent mirror is the last element of the optics and will be used for meridional focusing of the beam at the different sample positions. Therefore, the curvature radius should be varied between 8 and 12 km. The mirror serves to increase the flux on the sample and to adjust vertically the beam if needed. In addition, a non-dispersive mirror setting is proposed. Therefore, vertical movement of the beam, when the mirror incidence angle is changed, should be eliminated. In branch *B*, non-crystalline diffraction experiments will be possible by reducing the parasitic scatter with the aid of three slits: two collimating slits and a guard slit. The first collimating slit will be placed immediately after the last optical element, *i.e.* the second mirror, and will cut off any parasitic scatter due to any imperfections in the optics. The second collimating slit will be placed downstream as close as possible to the sample position so that the converging beam can be appropriately defined and, once again, the parasitic scatter removed. Finally, the guard slit will be placed immediately before

the sample so that any scatter coming from the edges of the second slit can be removed. This assembly defines the size of the beam spot and, therefore, the minimum observable diffraction/scattering angle (Bras *et al.*, 1993; Bosecke *et al.*, 1995).

The performance of the optical design has been checked by ray tracing using *SHADOW* (Lai & Cerrina, 1986). The calculation results for energy resolution, photon flux, and beam size in real and phase space shown in Tables 1 and 2 have been obtained for a photon energy of 12.4 keV and a ring current of 0.1 A. The source has been obtained from a 5000-ray random simulation, with a Gaussian space distribution and a synchrotron source depth.

### 3. Conclusions

A description of the optical layout of the Spanish beamline (SpLine) has been presented. The beamline will be installed on bending-magnet port B25 at the ESRF and has been conceived as multipurpose and interdisciplinary. By using the advantages of a wide front end (9 mrad), the Spanish beamline will be split in two branches with a fan of 2 mrad each, the central 5 mrad will be blocked. Each branch will be fully equipped with its own focusing optics and experimental stations, permitting measurements on each branch to proceed independently. The optics consist of two mirrors and a fixed-exit double-crystal monochromator (DCM). The horizontal focusing will be achieved by the second monochromator crystal through sagittal cylindrical bending. The beam can be focused vertically to different sample positions away from the source by a second vertically focusing mirror having a variable bending radius.

Special thanks are addressed to S. Ferrer, I. Kilvington, and many other ESRF and CRG staff members for very long and fruitful discussions. Additionally, I thank Manuel Sanchez del Rio for his help in the ray-tracing calculation.

### References

- Bosecke, P., Diat, O. & Rasmussen, B. (1995). *Rev. Sci. Instrum.* **66**, 1636–1638.
- Bras, W., Derbyshire, G. E., Ryan, A. J., Mant, G. R., Felton, A., Lewis, R. A., Hall, C. J. & Greaves, G. N. (1993). *Nucl. Instrum. Methods*, **A326**, 587–591.
- Hazemann, J. L., Nayouf, K. & de Bergering, F. (1995). *Nucl. Instrum. Methods*, **B97**, 547–550.

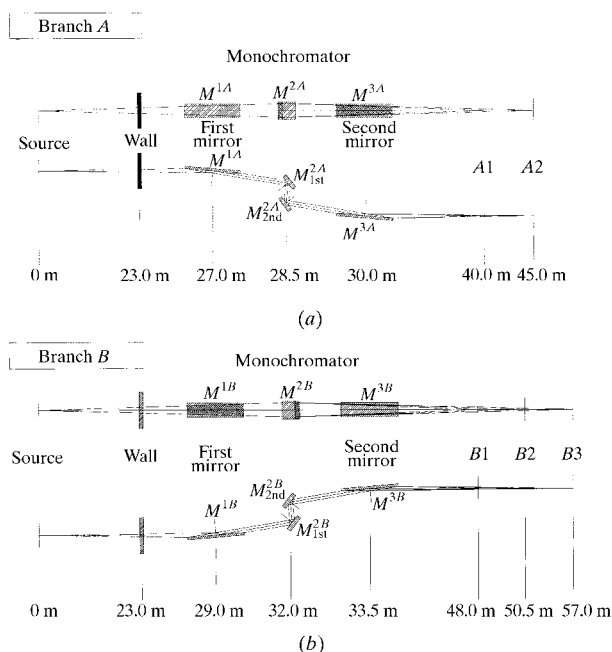


**Figure 3**  
(a) Schematic representation of beam path for the configuration of branch *A*. (b) Schematic representation of beam path for the configuration of branch *B*.

Heald, S. M. (1984). *Nucl. Instrum. Methods Phys. Res.* **222**, 160–163.

Kirsch, M., Freund, A., Marot, G. & Zhang, L. (1991). *Nucl. Instrum. Methods*, **A305**, 208–213.

Lai, B. & Cerrina, F. (1986). *Nucl. Instrum. Methods*, **A246**, 337.

Pascarelli, S., Boscherini, F., D'Acapito, F., Hrdý, J., Meneghini, C. & Mobilio, S. (1996). *J. Synchrotron Rad.* **3**, 147–155.